AIAA 96-0242

The Cassini INCA Sensor: Thermal Design, Analysis and Test

Edward 1. Lin, Ronald T. Reeve, Glenn T. Tsuyuki and James W. Stultz
Jet Propulsion Laboratory
California Institute of Technology
Pasadena, CA

34th Aerospace Sciences Meeting & Exhibit
January 15-18, 1996 / Reno, NV

THE CASSINI INCA SENSOR: THERMAL DESIGN, ANALYSIS AND TEST

Edward I. Lin*, Ronald T. Reeve', Glenn T. Tsuyuki+ and James W. Stultz&
Jet Propulsion Laboratory
California Institute of Technology
Pasadena, California

Abstract

Thermal design, analysis, and test of the Cassini ion and neutral camera are reported in this paper. The evolution of the thermal design is described, and analytical and test results are presented to show adequacy of the design. It is intended to illustrate that a correlated and synergistic approach to the design, analysis and test processes benefits spacecraft hardware development in an increasingly cost-conscious environment.

Introduction

The Cassini spacecraft is being developed for a mission to explore Saturn and its rings, satellites and magnetosphere. The MIMI-INCA (Magnetospheric IMaging Instrument - Ion and Neutral CAmera) sensor will be on board the Cassini spacecraft to investigate the dynamics of the ion and neutral species in Saturn's magnetosphere and study the coupling between the magnetosphere and the ionosphere. The processes and results of thermal design, analysis and test for the INCA sensor are described in this paper. Attention is drawn to the manner in which the three processes interacted with one another, and the importance of the test in validating the design and analysis.

Thermal Design

The INCA sensor is located on the upper shell structure assembly (USSA) of the Cassini spacecraft as shown in Fig. 1, with a close-up view shown in Fig. 2.

The sensor consists of the upper and lower electronics housing, made of magnesium, which houses the electronics and detectors, and a collimator which is supported by, but isolated from, the electronics housing. The collimator fins are alternately charged, separated from each other, and supported on the ends by G-10 brackets. The energetic neutral or ion species from the hot plasma in Saturn's magnetosphere enter via the gaps between the fins, pass through the aperture which is located at the top of the upper housing, and are registered at the solid state detector matrix.

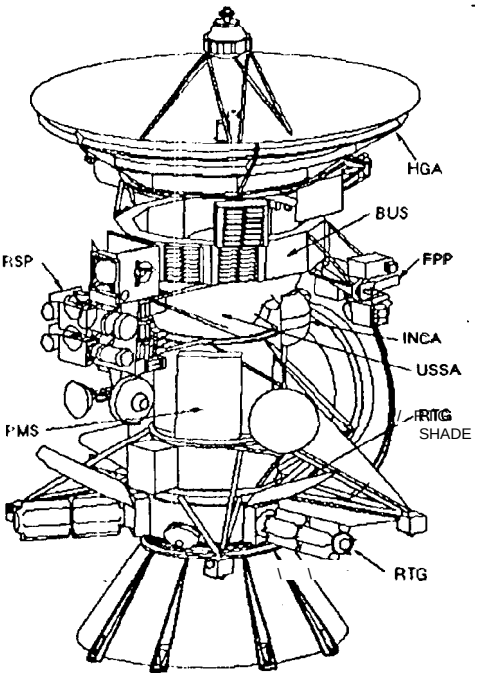

Fig. 1 INCA on tine Cassini spacecraft

The sensor is mounted on the USSA by means of three aluminum bipeds. The collimator front is exposed to space, but the sides are blanketed. The Propulsion Module Subsystem (PMS) blanket envelops a cavity around INCA, and under this blanket the upper and lower electronics housing views the USSA, the MIMI main

* Member of Technical Staff; Member AIAA
' Member of Technical Staff
'Technical Group Leader; Senior Member AIAA
'Acting Group Supervisor; Member AIAA

electronics, the hydrazine tank, and other neighboring subsystem... A sunshade extending from one of the collimator side plates provides protection against solar illumination during off-sun Trajectory Correction Maneuvers (TCMs).

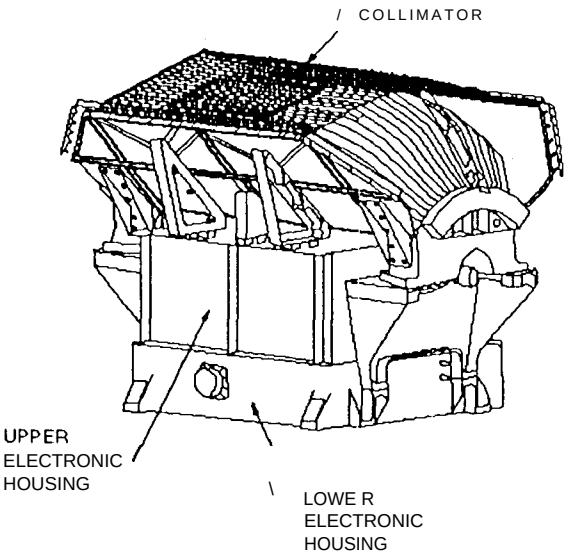

Fig. 2 The INCA sensor

The allowable flight temperature (AFT) requirements for the INCA sensor are: -20°C / + 35°C for min/max operation, and -25°C / +50°C for min/max non-operation. These requirements are applicable to the bulk average of the electronics housing. No specific temperature limits or temperature-gradient requirements have been deemed necessary for the collimator due to the nature of the design and intended operations.

The INCA thermal design seeks to achieve a proper level of coupling between the instrument and the USSA. Conductive coupling is accomplished by the aluminum support structure which consists of three bipeds. the associated fittings and an interface plate. Radiative coupling takes place between the electronics housing and the surrounding cavity. The neighboring subsystems inside the cavity, including the USSA, the MIMI main electronics, and the underside of the bus (painted black), present a generally warming influence on INCA. An earlier design utilized black paint on the electronics housing to maximize radiative coupling. However, the surface coating was later changed to DOW 15, for reasons explained in the analytical results section.

The initial design made provisions to install replacement, supplemental and decontamination heaters on the upper or lower electronics housing to keep the instrument within the allowable flight temperatures. The replacement heaters were to maintain the electronics housing above -25°C during the non-operating mode; the supplemental heaters were to maintain the housing above -20°C in the operating mode, including the sleep mode; and the decontamination heaters were to keep the housing temperature above + 20°C during decontamination. As reported in the following, both the analysis and test phases concluded that no replacement and supplemental heaters are necessary, and a 15 W heater is required for decontamination.

Analysis

Analytical Model

The SINDA model[1] is based on a reduced model constructed for the sensor proper, and includes a support structure model and various boundary condition representations obtained from pertinent neighboring subsystems. Note that the INCA sensor is designed and constructed by Applied Physics Laboratory (APL), and so is the reduced sensor model, The model is simple yet contains sufficient details for the intended purpose of calculating bulk temperatures. Some TRASYS models[2] of the collimator fins were also constructed to calculate the effective emissivity for the collimator that was incorporated into the reduced SINDA model.

As boundary conditions, the neighboring subsystems under the PMS blanket have been treated as a cavity effective sink. Both the USSA (conductive boundary) and the cavity effective sink temperatures have been derived from predictions by the spacecraft central body model. The overall thermal conductance of the biped support structure has been calculated considering all six struts, the fittings, and the various contact resistances at the bolted and bonded joints. Due to uncertainties associated with contact resistances and approximations of fitting geometries, a sensitivity range for the overall thermal conductance was also estimated.

Analysis Results

Analyses conducted include steady-state calculations for worst-case hot and cold, and nominal hot and cold conditions; heater sizing and heater power sensitivity calculations; sensitivity studies varying the overall thermal conductance between INCA and the USSA, the cavity effective sink temperature, the high-emissivity black paint vs. the low-emissivity DOW 15

coating, and some key boundary conditions. The results are presented in Table 1, where both key input parameters and computed temperatures are displayed.

Predictions for the lower electronics housing temperature indicate comfortable margins (greater than 11°C) relative to the AFT limits for both worst-case hot and worst-case cold conditions. An energy balance for the worst hot case indicates that the major heat flow paths are from the USSA and the PMS cavity to the electronics housing, and from tbe housing to the collimator then to space. Forheater sizing andheater power sensitivity, all runs were made under worst-case cold conditions. A decontamination heater size of 10W is required to maintain the electronics housing above 20°C. Although no replacement and supplemental heaters are required according to Case B1 (Table 1), these runs provide art insight into how the electronics housing temperature varies in response to heater power (roughly 3°C/W).

The overall thermal conductance between INCA and USSA includes uncertainty in the values of thermal conductivity and contact resistance, and in the estimation of area and length along the heat flow path. The thermal-conductance sensitivity studies show greater sensitivity in the cold case than in the hot case, but the lower electronics housing temperature varies no more than 3°C from nominal within the uncertainty band in all cases. The sensitivity study with regard to the cavity effective sink temperature indicates that for every 10"C variation in the cavity temperature, the lower electronics housing temperature will be affected by about 3°C (Fig. 3).

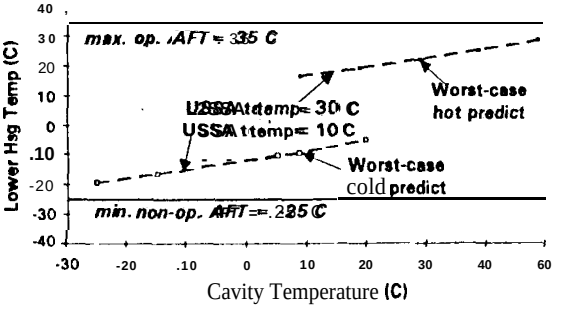

Fig. 3 INCA sensitivity to PMS cavity effective sink temperature

An earlier INCA design was baselined with a black paint on the housing to maximize the coupling between INCA and the spacecraft. However, subsequent analysis considering revisions in the key boundary temperatures and in the AFT requirements revealed that DOW 15 (ϵ = O. 13) is advantageous to black paint (ϵ = 0.87). The lower emissivity coating reduces decontamimtion heater power by 10 W, and reduces the instrument operating temperatures by 4 to 5°C thereby attenuating the detector noise. Cases El -E5 in Table 1 are to be contrasted with Cases Al -A4 and B6. This comparison is depicted in Fig. 4 by the bar in the middle and the bar on the right. The bar on the left recapitulates the pre-1994 design and analysis results to give a historical background. The design subjected to the thermal vacuum testing, reported below, is represented by the bar on the right, which illustrates that the design is within the AFT limits with comfortable margins.

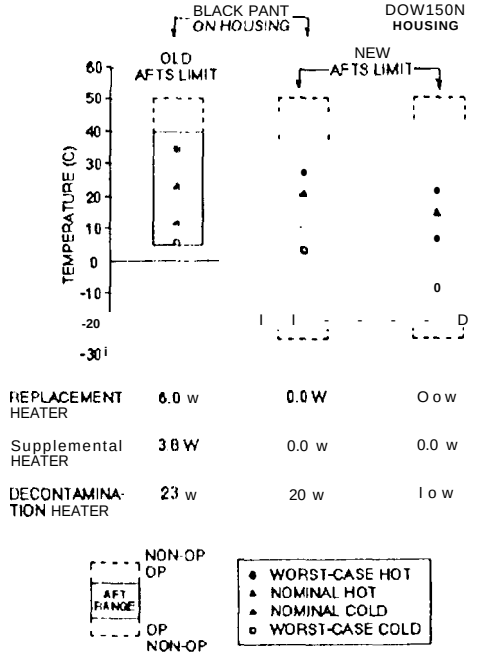

Fig. 4 Comparison of different INCA designs

Transient analyses include the case of a TCM with the spacecraft off the normaf sun-pointing configuration at 0.61 AU (2.7 suns exposure), the case of loss-of-sun-knowledge fault for a hypothesized 6-rein head-on solar illumination, and a post-launch cooldown simulation. The TCM transient simulation at 0.61 AU starts with the worst-case hot initial conditions. The 2.7-sun irradiance is imparted on the side of the collimator which is protected by the sunshade. The event is projected to last 30 ruin, but the simulation was run for 1 hr. The

results show that the sunlit MLI outer layer temperature rises to 186°C, the sun-side collimator side plate temperature rises from 6°C to 40°C, and the lower electronics housing temperature increases from 22°C to only 23°C. All temperatures are within AFT requirements and material limits.

The simulation for the loss-of-sun-knowledge fault at 0.61 AU (closest solar approach for the design) also starts with the worst-case hot initial conditions. The 2.7 suns illuminate the collimator head-on beaming down the instrument boresight. 'The simulation results show that the lower electronics housing temperature is hardly raised during the first 6 min. The collimator temperature is predicted to increase from -91°C to -81°C after 6 min. and to 4°C after 1 hr. However, it was recognized that these transient predictions based on a lumped-parameter one-node treatment for the collimator are not meaningful. In reality, the gold-plated thin fins individually should have fast response to the transient event, but the fin temperature determination is best left to test than to elaborate modeling. For the transient response during post-launch cooldown, the simulation starts with a uniform temperature of 15°C for the instrument and spacecraft, all power being turned off. The event is projected to last no longer than 2 hours but the simulation was run for an additionat hour. The results indicate that the lower electronics housing cools to 6°C after 2 hours, well within the AFT limits.

Thermal Vacuum Verification Test

Test Article, Setup and Procedure

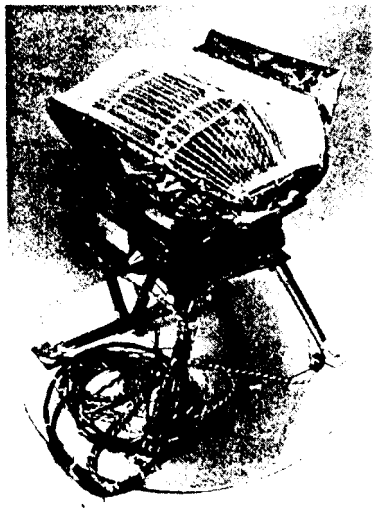

Fig. 5 INCA sensor test article

A thermal development test was conducted to verify the adequacy of the INCA thermal design and to help size the heaters[3]. The INCA sensor test article, shown in Fig. 5, is supported on three bipeds which are bolted to a round flat plate simulating the USSA. Fig. 6 shows the test article after it has been wrapped in the M LI blanket which created the simulated PMS cavity around the sensor. The bipeds, the flat plate and the cavity were all expedient approximations, and were intended to reduce cost and slightly cold-bias the test setup. The sensor thermal development model (TDM) was provided by APL and also contained some substitutes; e.g., the collimator fin material was aluminum instead of AlBuMet. NO electronics were included with the TDM; the electronics power dissipation was simulated by using the replacement heaters. These and other deviations from flight configurations were expected to have minor effects on the test results. Sensitivity studies were conducted before the test with the aid of the SINDA model to bound the effects of these approximations. For example, hypothetical variations on the bipeds' thermal conductance were shown to produce a change in the lower housing temperature of no greater than 3°C, and a change in the heat flow from the USSA to the sensor of no greater than 0.3 w.

Fig. 6 Test assembly ready for installation in chamber

Kapton etched foil heating elements were mounted on the upper and lower electronics housing to simulate the replacement, supplemental, and decontamination heaters. Six film heaters were mounted on the USSA simulation plate, and a guard heater was applied to the heater and thermocouple wire bundle where it exited from the PMS cavity near the USSA simulator plate. More than 40 Type E (Chromel constantan)

thermocouples, gage 26 or 30, were placed on various parts of the sensor and support structures, as well as the chamber shroud.

The test was performed in a 3-ft-diameter horizontal chamber. The test assembly (Fig. 6) was a tight fit in the chamber and was suspended with stainless steel wires from the chamber top rail at two places, one around the upper housing, and the other from the top of the USSA plate, with the configuration in Fig. 6 turned 90° such that the collimator faced the chamber door, which had a quartz window to admit' light from a solar simulator located outside the chamber.

There were three test phases. The first phase verified the thermal design under the worst-case hot and cold conditions, sized the heaters, and performed sensitivity studies. All tests were conducted with the chamber shroud at LN_2 temperature, chamber. pressure at less than 1 $x10^{-5}$ torr, and with the heater powers adjusted to facilitate reaching the target steady state. Steady state was assumed to be attained if temperatures changed at a rate of no greater than 0.2°C/hr. The second phase started with a post-launch cooldown simulation which lasted for a conservative period of 8 hours, and followed by an off-sun TCM simulation. For the latter, a heat shroud was installed near one side of the collimator to drive the outerlayer of the "sunlit" collimator MLI to a temperature of greater than 250°C. The TCM simulation started from a hot steady state and lasted for a conservative period of 2 hours. The third phase simulated a loss-of-sun-knowledge fault condition, with the solar simulator illuminating the collimator fins head-on with a 2.7-sun irradiance for a duration of 27 rein, which was conservatively longer than the required 6 minutes. Attention was focused on the aperture foil temperature as well as the fin temperatures during this phase.

Test Results

The thermal development test accomplished all the test objectives. The INCA thermal design was verified to be sound and robust, capable of satisfying all the thermal requirements under the worst-case conditions with comfortable margins. The test concluded that the replacement and supplemental heaters can be eliminated (which were initially allocated 10.9 W and 7.0 W, respectively), and that the decontamination heater power can be reduced (from the initial 18.75 W to 15.0 W). Conservative, extended simulations of the post-launch cool-down, the off-sun TCM and the loss-of-sun-knowledge fault conditions at 0.61 AU revealed no problems. The replacement of black paint by the DOW 15 coating on the electronics housing was proven beneficial, and transient data collected for the collimator fins and aperture foil provide valuable insight into their thermal behavior under extreme conditions. Some key test results are described as follows.

Figure 7 summarizes the steady-state temperatures obtained from the test for the lower electronics housing. Data points A through E are derived from the following test conditions:

A: Worst-case hot (INCA operating at 3.1 W, hot USSA at 32°C)

B: Worst-case cold (INCA non-operating, cold USSA at 8°C)

c: "Replacement heater sizing" (INCA non-operating, replacement heater at 2.5 W, cold USSA at 10"C)

D: "Decontamination heater sizing" (INCA non-operating, decontamination heater at 13.5 W, cold USSA at 10°C)

E: Hot sensitivity (INCA operating at 3.1 W, hypothetically hot USSA at 46°C)

F: Cold sensitivity (INCA non-operating, hypothetically cold USSA at 1°C)

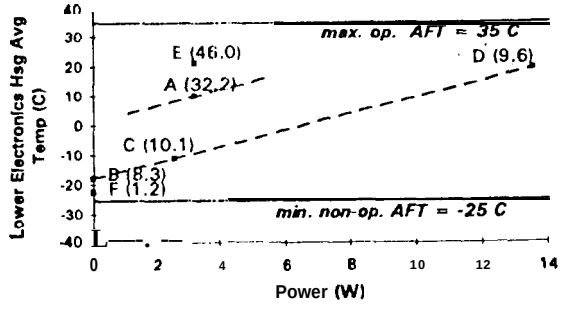

Fig. 7 MIMI-INCA steady state test temperatures (Number in parentheses denotes average temperature of USSA simulation plate in deg. C)

The results in Fig. 7 are presented in terms of the average lower electronics housing temperature, noting that the average upper electronics housing temperature is typically 1 to 2°C cooler. A comparison of these test results and the AFT's indicates comfortable design margins both on the hot and cold sides. The worst hot case result (Data point A) indicates a 25°C margin, and the worst cold case result (Data point B) indicates a margin of 8"C.

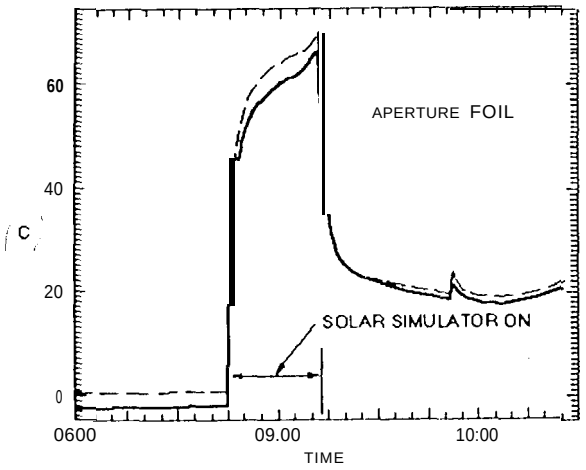

Fig. 8 Aperture foil temperature during 2.7-sun illumination test

Data point B (Fig. 7) shows that the thermal design is viable for the worst-case cold conditions even without replacement and supplemental heaters. Data point C indicates that the application of 2.5 W of heater power will increase the lower electronics housing temperature by 7°C. Data point F shows that even if the USSA temperature dropped down to an unrealistically low 1°C, the lower electronics temperature was still 2°C above the minimum non-operating AFT. Noting that the warming effects of the surrounding subsystems (e.g., RSP, MIMI main electronics, etc.) (was) absent from the small simulated **PMS cavity, and that the three test bipeds were** somewhat cold-biased in their deviation from the flight configuration, these non-operating cold-case tests clearly point to the conclusion that replacement and supplemental heaters are unnecessary. This corroborates with the analytical predictions. In fact, the last two observations (i.e., cold-biased bipeds and absence of the surrounding warm instruments) probably account for the fact that the test results are lower than the analytical predictions by about 8°C in the cold case and by about 1 l°C in the hot case. Also, data points E and A show that dT_{INCA}/dT_{USSA} · 12°C/140C, and data points B and F show that dT_{INCA}/dT_{USSA} - 5°C/7°C, indicating a high INCA sensitivity to the USSA temperature. Data point D indicates that a 13 .5 W heater (as opposed to the predicted 10 W, due to the cold bias) is almost sufficient for decontamination purposes. With a little extrapolation, it is evident that a 15 W decontamination heater is sufficient to keep the electronics housing above the desired 20°C.

The transient test phases covered the post-launch cooldown, the spacecraft off-sun TCM, and the loss-of-sun-knowledge fault simulation. The test conditions were conservative, and all results indicate that the AFT requirements are satisfied. For example, Fig. 8 presents the aperture foil temperature transients occurring during a 2.7-sun exposure. Inspection after the test showed that the "thermal shock" did not damage the foil. Figure 9 shows how key INCA components responded to the 2.7-sun illumination. While the thin collimator fins rose sharply to above 80°C, the lower electronics housing stayed "below 23°C at the end of the conservative 27-min. exposure period. The USSA behavior shown in Fig. 9 is not representative of the real system because it has a much greater thermal mass in the flight configuration than in the test assembly.

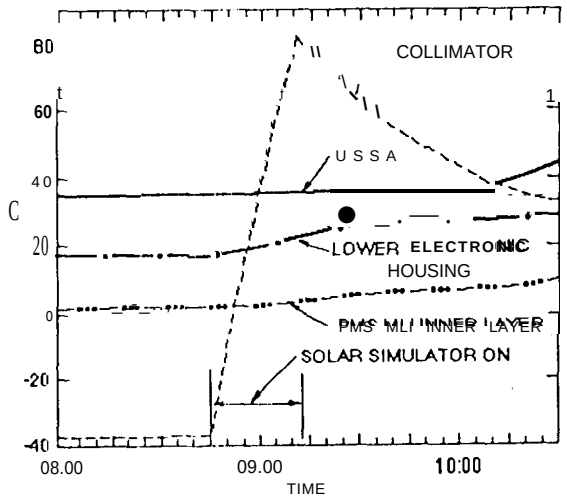

Fig. 9 Transient temperature response of key INCA components during 2.7-sun illumination test

Collimator Design Change and Sensor Relocation

Collimator design change

Subsequent to JPL's thermal development test, it was determined by APL during a sensor performance test that the original gold plated AlBuMet fins would not support high voltage without arcing. Furthermore, the thickness of the fin plate smoothed over the sharp-cornered ribs on the plate. The fin material was changed from AlBuMet to Magnesium AZ31B-H24, the gold coating was replaced by Irridite 15 to maintain sharp comers on the fin ribs, the fins became longer and narrower (by less than 1"), and the side plates and end caps were modified. Although there were quite a number of design changes, APL conducted analysis and test to make sure that these

changes caused no adverse thermal effects. For example, in the thermal development test conducted by JPL, aluminum fins were used in the APL-provided TDM. When the collimator was exposed to 2.7 suns, the TDM tin temperature rose at a rate of 5°C/min. APL determined that a change of fin material to magnesium will increase the temperature rise rate to 7 .5 °C/min which is still acceptable for the postulated 6-rein loss-of-sun-knowledge fault. APL's test also indicated that the fin coating change results in a small increase in heat loss (less than 2 W) from the sensor, causing no violation of any temperature requirements .

Sensor Relocation

In addition, JPL investigators found that the old INCA conjuration interfered with the stray light field-of-view of the UltraViolet Imaging Spectrometer Subsystem (UVIS), which is located on the RSP. This necessitated a relocation of INCA and several constraints must be satisfied, including field-of-view requirements concerning LEMMS, the HGA and RTG3. The relocation involved a circumferential shift of the sensor by approximately 5", and a movement of the sensor closer to the USSA by approximately 3.5", plus a slight rotation. The dimensional changes would not show in the scale of Fig. 1, but the attendant changes in the lengths and wall thicknesses of the support struts caused a 14-18% increase in the overall thermal conductance between the sensor and the USSA. The INCA external radiation environment was not significantly affected by the relocation.

Using the revised SINDA model which reflects the design changes, several key cases were reanalyzed. The results for the worst hot and cold cases and the decontamination heater sizing run, are presented in the bottom shaded portion of Table 1. It is seen that the lower electronics housing temperature is still well within the AFT requirements, and the 15 W decontamination heater power remains valid for the modified INCA. In fact, comparing with previous analytical results, shown in the upper part of the same table, the lower electronics housing temperature is higher now by 0.5°C in the worst hot case, and higher by 2.3°C in the worst cold case. In other words, the collimator design changes and the INCA relocation together produce minimal temperature effects on INCA, as APL has shown by analysis and test investigating the effects of collimator design change alone.

Conclusions

The processes and results of thermal design, analysis and test for the Cassini MIMI-INCA sensor have been presented. As typical with any complex spacecraft subsystem, these processes have been evolutionary and interactive, The verification test not only serves the important purpose of ensuring that the design and analysis are adequate, but also makes it possible to avoid overly elaborate analysis. On the other hand, pre-test sensitivity analysis enables simplification of test configurations and procedures, and post-test analysis helps m the interpretation of the test results. The correlated and synergistic approach to the design, analysis and test processes, taken here for the development of INCA, appears to be a beneficial one in art increasingly cost-conscious environment. The result of this approach is a sound and robust thermal design that will satisfy the temperature requirements necessary for the study of the ion and neutral species in Saturn's magnetosphere.

Acknowledgment

The work described in this paper was carried out by the Jet Propulsion Laboratory, California Institute of Technology, under a contract with the National Aeronautics and Space Administration. The authors appreciate the cooperation and assistance provided by the following JPL personnel during the thermal development test: J. Real, T. Fisher, P. Martin, G. Laugen, E. Bailey, D. Perry, R. Okamoto, L. Johnson , and H. Winter. System engineers M. Marshall (JPL) and S. Jaskulek (APL) have been instrumental in facilitating the inter-agency interface. D. Mehoke has been the responsible APL thermal engineer whose technical work and cooperation have been essential for the development of this sensor.

References

1. E. I. Lin, "Cassini MIMI-INCA Thermal Design, Model, and Analysis, " JPL Interoffice Memorandum 3544-CAS-94-179, Oct. 7, 1994.

2. D. S. Mehoke (APL), private communication, Sept. 1994.

3. E. 1. Lin, "Cassini MIMI-INCA Thermal Development Test Report," JPL Interoffice Memorandum 3544-CAS-95-02 1, Feb. 8, 1995.

Table 1. MIMI-INCA Analysis Results

Rsm case	Case Conditions	Input Parameters: USSA T (C)	Cavity T (C)	MLI outer T (C)	Bipeds Cond. (W/C)	MLI eff. E	Electr. Hous'g E	Oper. Power (W)	Heater Power (W)	Computed Temperature (C): Lower Hous'g	Upper Hous'g	Colli-mater	End Supp't	Clmtr Side Plate	Remarks
Worst-Case Hot and Cold: Nominal Hot and Cold															
A1	Worst-Case Hot	30	29	-110	0.224	0.01	0.13	3.13	0	22.2	20.1	-91.1	-43.8	6.4	min/max op AFT
A2	Worst-Case Cold	10	8	-130	0.139	0.04	0.13	0		-9.5	-11.9	-109.8	-61.6	-25.3	are -20/+35 C;
A3	Nominal hot	25	23	-120	0.167	0.025	0.13	3.13		15.3	13.2	-95.3	47.9	-2.4	min/max non-op
A4	Nominal cold	15	12	-120	0.167	0.025	0.13	3.13		6.7	4.8	-100.1	-52.2	-9.2	AFT are -25/+50 C
Heater Sii and Heater Power Sensitivity															
B1	worst-Case Cold	10	8	-130	0.139	0.04	0.13	0		-9.5	-11.9	-109.8	-61.6	-25.3	
B2	Replacement Heater							o	2W@#2	-2.8	-4.4	I-105.6	I-57.7	-19.3	
B3	Supplemental Hearer							2.22	1W@#2	1.!	0	-103.1	-55.4	-15.7	
B4	Heater Power Sensitivity							o	4W@#2	3.5	2.8	-101.5	-53.9	-13.5	
B5	Heater Power Sensitivity							o	8W@#2	15.6	16.4	-93.9	47.1	-2.9	
B6	Decontamination Htr.							0	10W@2	21.3	22.9	-90.3	43.9	2.1	
Sensitivity Study - Overall Thermal Conductance Between INCA and USSA															
C1	Hot	30	29	-110	0.224	0.01	0.13	3.13	0	22.2	20.1	-91.1	-43.8	6.4	Note: A blank
C2	Hot				0.167					20.9	18.9	-91.8	-44.4	5.4	parameter entry
C3	Hot				0.139					20.1	18.2	-92.2	-44.7	4.8	assumes the same
C4	Cold	10	8	-130	0.139	0.04	0.13	0		-9.5	-11.9	-109.8	-61.6	-25.3	value as the one
C5	Cold				0.167					-7.7	-10.2	-108.9	-60.7	-24	immediately above
C6	Cold				0.224					4.9	-7.7	-107.4	-59.3	-21.9	throughout table
sensitivity Study - Cavity Effective Sink Temperature															
D1	Hot	30	39	-110	0.224	0.01	0.13	3.13		25.4	23.4	-89.2	-42.1	9.2	
D2	Hot		29							22.2	20.1	-91.1	-43.8	6.4	
D3	Hot		19							19.4	17	-92.8	-45.3	3.8	
D4	Cold	10	20	-130		0.04	0.13	0		-5	-7.3	-107.2	-59.1	-21.6	
D5	Cold		8							-9.5	-11.9	-109.8	-61.6	-25.3	
D6	Cold		-15							-16.8	-19.6	-114.1	-65.7	-31.6	
Black Paint on Electronics Housing (Instead of DOW 15)															
E1	Worst-Case Hot	30	29	-110	0.224	0.01	0.87	3.13		27	25.4	-88.1	-41.1	10.8	
E2	Worst-Case Cold	10	8	-130	0.139	0.04	0.87	0		2.6	0.8	-102.6	-54.9	-1.5.	
E3	Nominal Hot	25	23	-120	0.167	0.025	0.87	13.13		20.9	19.3	-91.9	-44.9	2.4	
E4	Nominal Cold	15	12	-120	0.167	0.025	0.87	3.13		10.6	9.1	-97.7	-49.9	-5.8	
E5	Decontamination Htr.	10	8	-130	0.139	0.04	0.87	0	20W	21.2	25.1	-89.1	-42.8	13.7	
Nominal Case Predicts (Varying USSA & Cavity Temperatures)															
F1	Hot	30	29	-120	0.15	0.025	0.13	3.13	0	19.3	17.1	-93.1	-45.9	0.7	
F2	Hot	25	23					3.13		14.8	12.8	-95.6	-48.1	-2.8	
F3	Cold	15	12					3.13		6.2	4.4	-100.3	-52.4	-9.6	
4	Cold ,	10	8					0		7.8	10.2	-108.5	-60	-21.6	
Analysis pursuant to Relocation and Collimator Change															
A1-R	Worst-Case Hot	30	29	-110	0.264	0.01	0.13	3.13	0	22.7	20.3	-94.9	-36.5	-2.6	
A2-R	Worst-Case Cold	10	8	-130	0.158	0.04	0.13	0	0	-7.2	-9.9	-112.4	-55.1	-31.2	
B6-R	Decontamination Htr.	10	8	-110	0.264	0.01	0.13	o	15W@2	27.6	32.1	-88.4	-30.1	6.1	